

The M31 Globular Cluster Luminosity Function¹

Pauline Barmby²& John P. Huchra

Harvard-Smithsonian Center for Astrophysics, 60 Garden St., Cambridge, MA 02138

pbarbmy@cfa.harvard.edu, huchra@cfa.harvard.edu

and

Jean P. Brodie

Lick Observatory, University of California, Santa Cruz, CA 95064

brodie@ucolick.org

ABSTRACT

We combine our compilation of photometry of M31 globular clusters and probable cluster candidates with new near-infrared photometry for 30 objects. Using these data we determine the globular cluster luminosity function (GCLF) in multiple filters for the M31 halo clusters. We find a GCLF peak and dispersion $V_0^0 = 16.84 \pm 0.11$, $\sigma_t = 0.93 \pm 0.13$ (Gaussian $\sigma = 1.20 \pm 0.14$), consistent with previous results. The halo GCLF peak colors (e.g. $B_0^0 - V_0^0$) are consistent with the average cluster colors. We also measure V -band GCLF parameters for several other subsamples of the M31 globular cluster population. The inner third of the clusters have a GCLF peak significantly brighter than that of the outer clusters ($\Delta V^0 \approx 0.5$ mag). Dividing the sample by both galactocentric distance and metallicity, we find that the GCLF also varies with metallicity, as the metal-poor clusters are on average 0.36 mag fainter than the metal-rich clusters. Our modeling of the catalog selection effects suggests that they are not the cause of the measured GCLF differences, but a more-complete, less-contaminated M31 cluster catalog is required for confirmation. Our results imply that dynamical destruction is not the only factor causing variation in the M31 GCLF: metallicity, age, and cluster initial mass function may also be important.

Subject headings: galaxies: individual (M31) – galaxies: star clusters – globular clusters: general

¹Based partially on observations made with the NASA/ESA Hubble Space Telescope, obtained from the data archive at Space Telescope Science Institute. STScI is operated by the Association of Universities for Research in Astronomy, Inc. under NASA contract NAS 5-26555.

²Guest User, Canadian Astronomy Data Centre, which is operated by the Herzberg Institute of Astrophysics, National Research Council of Canada.

1. Introduction

Globular clusters (GCs) are unique markers of the formation and evolution of galaxies. They are bright, easily identifiable packages of Population II stars with homogeneous abundances and history. GCs are relics of the earliest star formation in galaxies and have witnessed many changes in their parent galaxies. The study of globular cluster systems (GCSs) is thus important in understanding the history of galaxies.

The distribution of integrated GC magnitudes, known as the globular cluster luminosity function (GCLF), has long been known to be unimodal and approximately symmetric in the Milky Way. The assumption that these properties are universal has allowed the determination of GCLF parameters for over a hundred other galaxies, and the peak absolute magnitude is found to be roughly constant from galaxy to galaxy (Harris 1988). Since the variation in mass-to-light ratios among GCs is fairly small (see, e.g., Dubath & Grillmair 1997) the constant peak magnitude implies the existence of a characteristic mass scale. Theorists have attempted to explain why there should be a characteristic mass scale for globular clusters: is it a property of formation (e.g. Peebles & Dicke 1968), a result of subsequent dynamical processes (e.g. Okazaki & Tosa 1995), or a combination? The constant peak magnitude also presents a challenge to observers, who have attempted to quantify the variation in peak magnitude by environment (Blakeslee & Tonry 1996), galaxy type and luminosity (Whitmore 1997), and color (Kundu et al. 1999). Many observers have also attempted to use the GCLF peak as a standard candle for distance measurement. This method has had a mixed reception, with some authors (e.g. Whitmore 1997) claiming good results and others (e.g. Ferrarese et al. 2000) less complimentary.

GCLF measurements are made in a number of different bandpasses. The most widely used are V and B , (and their Hubble Space Telescope (HST) equivalents, F555W and F450W); the I-band equivalent F814W is also commonly used for HST data. B and V band mass-to-light ratios are sensitive to metallicity, so GCSs with the same underlying mass distribution but different average metallicities will have different GCLFs. Ashman, Conti, & Zepf (1995) used the relation between metallicity and mass-to-light ratio as predicted by Worthey’s (1994) simple stellar population models to estimate the effects of metallicity variations on the GCLF peak. Metal-rich clusters should be fainter (their M/L is larger), and the effect on the GCLF can be substantial. For example, Ashman et al. (1995) predict that a change in mean GCS metallicity from $\overline{[\text{Fe}/\text{H}]} = -1.35$ dex (the Milky Way value) to -0.60 dex (the value for the elliptical NGC 3923; Zepf et al. 1995) shifts the GCLF peak by $\Delta B^0 = 0.35$ and $\Delta V^0 = 0.22$. The same metallicity change shifts the J band GCLF peak by $\Delta J^0 = -0.09$, because the metallicity effect on M/L changes direction for bandpasses redward of I . Observing at longer wavelengths also reduces the effects of extinction, both Galactic and within the GCS parent galaxy.

Destruction of globular clusters through dynamical effects could produce a globular cluster mass function (GCMF) that varies with distance from the center of the host galaxy. The three effects usually considered by modelers are disk shocking, evaporation, and dynamical friction; the

first two destroy low-mass, low-concentration clusters, while the last is most effective for massive clusters. All three effects are strongest at small Galactocentric distance R_{gc} . Even at small R_{gc} , the dynamical friction timescale for typical-mass GCs is much longer than a Hubble time, and dynamical friction is probably not important in GCMF evolution (Okazaki & Tosa 1995). Low-mass clusters near the Galactic center are thus most prone to destruction. Assuming a mass-to-light ratio independent of R_{gc} – if the GCS has a radial metallicity gradient this is not strictly true since M/L depends on $[\text{Fe}/\text{H}]$ – the radial difference in the GCMF can be translated into a radial difference in the GCLF. Many authors (Baumgardt 1997; Ostriker & Gnedin 1997; Vesperini 1998) have predicted the size of the GCLF variation, with widely differing results (see Section 4.3).

In Barmby et al. (2000) we compiled the best available photometry for 435 M31 globular clusters and plausible candidates. This catalog contains V magnitudes for almost all objects and B magnitudes for about 90%, but completeness in the longer-wavelength bands is much lower. About 55% of the objects have I magnitudes, and the same fraction, although not the same objects, have JK ; Figure 1 shows the completeness of the existing IR photometry. In this paper we estimate the parameters of the halo clusters’ GCLF in six different bandpasses; this includes the first GCLF measurements in the near-IR. We then investigate the variation in the V -band GCLF parameters for several different subsamples of M31 GCs. Finally, we consider the implications of the measured GCLF variations for GCS and galaxy formation and evolution.

2. New observations and data reduction

We obtained new near-IR photometry for M31 GCs and candidates using two telescope/instrument combinations: Gemini (McLean et al. 1994) on the Lick Observatory 3-m telescope, and Stelircam (Tollestrup & Willner 1998) on the F. L. Whipple Observatory 1.2-m. The Lick observations (in J , H and K') were made on 1999 October 15-17 and the Whipple observations (in J and K) on 1999 December 26. Total integration times ranged from 90 seconds (re-observations of bright clusters in J with Gemini) to 1900 seconds (observations of the faintest halo clusters with Stelircam), using 4 to 9 dithered frames per object.

We used almost the same data reduction procedure for both cameras, which consisted of bias-subtraction (Gemini only), dark-frame subtraction, non-linearity correction (Stelircam only), flat-fielding (using a ‘superflat’ made from 50-100 blank-sky frames), sky-subtraction, registration, and co-addition. Two methods of sky-subtraction were used: for objects on the galaxy disk we made separate sky observations and subtracted their median, and for objects without galaxy background we subtracted a ‘running sky’ made from the median of 4-8 temporally contiguous frames. We measured large-aperture magnitudes for Elias et al. (1982) and Persson et al. (1998) standard stars, typically 10-15 stars per filter per night, and fit a two-component (zeropoint and airmass coefficient) photometric solution using standard star magnitudes. Residuals of the photometric solution were typically about 0.01 – 0.02 mag. The difference between K and K' magnitudes of standard stars is smaller than these residuals (M. Pahre, 2000, private communication), so we

assume that our K' measurements adequately represent the K -band.

Our previous aperture photometry of globular clusters used 12-arcsec diameter apertures, and we found that, for the Gemini and Stelircam data, this aperture again contained about 95% of the total cluster light. The new measurements appear in Table 1. Some of these data are for objects whose previous IR photometry disagreed strongly with their spectroscopic metallicities (mostly blue clusters in Barmby et al. 2000); our new measurements yielded colors more consistent with the spectroscopic data. The original goal of these observations was to complete the IR photometry for the M31 halo sample of Reed, Harris, & Harris (1994). Poor observing conditions prevented us from completing the halo sample but we did obtain new photometry for 38 objects in total. The total number of M31 clusters and cluster candidates with JK photometry is now ~ 250 , including the 30 objects measured for the first time in this paper.

3. Preliminaries to the GCLF

3.1. Sample definitions

The standard approach to correcting for incompleteness and contamination in the GCLF (see, e.g., Forbes et al. 1996) is not feasible for M31. Our catalog is a compilation of several previous cluster searches, each with different sky coverage and selection functions. Foreground contamination is a more severe problem for M31 than for more distant galaxies: because M31 is nearby, it covers a large angular area and its GCs have apparent magnitudes comparable to those of Galactic stars. A list of ‘failed’ M31 GC candidates in Barmby et al. (2000) shows that about 15% are foreground stars. Other possible contaminants are background galaxies and objects such as open clusters and H II regions in the galaxy itself. Spectroscopy or high-resolution imaging are the only ways to unambiguously discriminate M31 GCs from contaminating objects, but these techniques have been used mostly on the brighter clusters (see Section 4.2). Battistini et al. (1987), the major source of clusters and candidates for our catalog, estimate that 80-90% of their probable (class A and B) cluster candidates with $V < 18$ are true M31 GCs.

Defining a complete, uncontaminated sample of M31 clusters to a magnitude limit well past the GCLF turnover is not possible with currently available data. There is no quantitative estimate of either the completeness or contamination rate, and any attempt to estimate these from the confirmed clusters is hampered by the strong dependence of both completeness and contamination on apparent magnitude and position in the galaxy. To reduce these effects as much as possible while still retaining a reasonable sample size, we define our ‘full sample’ to be all clusters in the Barmby et al. (2000) catalog with $V < 18$, $B - V > 0.45$, and $R > 5'$, where R_{gc} is the projected distance from the center of M31. The magnitude criterion restricts the sample to the range where incompleteness and contamination should be minimal. The color criterion is needed to remove objects in M31 which are bluer than any Galactic globular cluster and may possibly be younger clusters. We use here a slightly less stringent color criterion than in Barmby et al. (2000) in

order to retain as many of the halo clusters as possible; many of them are slightly (~ 0.02 mag) bluer than the previous limit of $B - V = 0.55$. Restricting the sample to $R > 5'$ also aims to reduce the incompleteness and contamination, as the bright galaxy background near the M31 bulge makes cluster identification and confirmation more difficult. Several groups (Wirth, Smarr, & Bruno 1985; Aurière, Coupinot, & Hecquet 1992; Battistini et al. 1993) have attempted to define a complete sample of GCs near the M31 nucleus. However, the published catalogs are likely to be both contaminated and incomplete: Barmby et al. (2000) showed that many of the objects listed by Battistini et al. (1993) are not globular clusters, and Mostek et al. (1999) recently identified 33 previously unknown GC candidates in the M31 bulge.

Our full sample has a total of 294 clusters and cluster candidates. The overlap with Battistini et al.’s (1993) ‘adopted best sample’ is about 85%; the differences are largely due to our exclusion of GCs with $R_{gc} < 5'$ and Battistini et al.’s use of a red color limit. To investigate the effects of metallicity on the GCLF, we define metal-poor (MP) and metal-rich (MR) subsamples by splitting the full sample at $[\text{Fe}/\text{H}] = -1.0$. Metallicities for most objects without spectroscopic data were estimated from colors as in Barmby et al. (2000); we accounted for clusters without metallicities by modifying the completeness functions. The metal-rich subsample has 75 objects and the metal-poor has 191. For comparison with the halo sample (see below), we define a disk sample consisting of all objects in the full sample which are not members of the halo. There are a total of 226 ‘disk’ objects (the number of disk plus halo objects is greater than the number of objects in the full sample because 18 halo objects have $V > 18$).

Measuring the GCLF of halo GCs in M31 avoids the problem of having to determine individual extinctions for each cluster, since these clusters should be subject to only foreground extinction. Racine (1991) began a concerted effort to define a sample of GCs in the M31 halo that was complete to a faint magnitude limit ($V \approx 19$) and free of contamination. He defined the halo boundary as a $260' \times 56'$ ellipse with position angle 38° , centered on the M31 nucleus (see Figure 1). The effort to produce a complete, uncontaminated halo sample was continued by Reed, Harris, & Harris (1992), Racine & Harris (1992) and Reed et al. (1994), and culminated in the published GCLFs of Secker (1992), Secker & Harris (1993, hereafter SH93), and Reed et al. (1994). Because of this work, incompleteness and contamination are much less severe for the halo clusters than for the overall population of GCs in M31. To construct our halo sample, we start with the sample of Reed et al. (1994). We remove the following three objects (see Barmby et al. (2000) for our naming convention) as probable non-clusters:

- 168D-D020: “probably not a cluster” (Battistini et al. 1987)
- 109D-000: suspected to be foreground star by both Battistini et al. (1987) and Reed et al. (1994)
- 007-059: shown spectroscopically to be a foreground star (Barmby et al. 2000)

Some of the GCs around M31 are near its companion, the dwarf elliptical NGC 205; the

clusters’ formation and evolution may have been influenced by NGC 205’s presence as well as that of M31. There is some evidence that the GCLF peak absolute magnitude in dE galaxies is fainter than that in large galaxies (Durrell et al. 1996; Harris 2000), so we attempt to remove these ‘contaminating’ objects from the M31 halo sample. We follow Reed et al. (1992) in considering 011-063, 324-051, 331-057, and 330-056 to be ‘NGC 205 clusters’ and dropping them from the M31 halo. We also remove three additional clusters from the M31 halo list:

- 328-054: very close to NGC 205 in both position (1.2’) and radial velocity (18 km s⁻¹)
- 326-000, 333-000: both < 2’ (400 pc) from NGC 205. No radial velocity information is available for these objects, and their projection onto NGC 205 also makes accurate photometry difficult.

We add 227-000 to our list, although Reed et al. (1992) reject this object from their halo sample because of its previous photometry. The rejection appears to have been a mistake, since their observations of this object put it within their color and curve-of-growth acceptance criteria. Our final halo list has 86 objects. The list used by Secker (1992) has 82 objects, as he excludes some ‘low-probability’ objects (469-220, DAO054, DAO055, DAO094, 456-000) while we retain these for the sake of completeness. The faintest object in our halo sample has $V = 18.98$, and we believe the sample to be essentially complete. Our catalog is probably missing a few distant, Palomar-type clusters in the M31 outer halo, but no M31 GC survey yet performed would have revealed such objects. (Finding Palomar-type GCs in M31 would require surveys to $V \approx 22$, in excellent seeing, to a radius of 5 degrees from M31.) In any case, the luminosity function should be little affected by the presence or absence of a few clusters far from the LF peak.

3.2. Extinction correction

One of the major problems with using the Milky Way and M31 globular cluster systems to calibrate the GCLF is the uncertain effect of extinction. Many of the Galactic GCs are in the Galactic plane and are highly extinguished; however, at least for those clusters the extinction can be determined from the color-magnitude diagram (CMD) and spectroscopy of individual stars. In M31, globular clusters’ CMDs are not precise enough for determination of extinction, and only about a dozen clusters have published CMDs. Instead, measurements of extinction for individual clusters (Vetešnik 1962; Crampton et al. 1985; Sharov & Lyutyi 1989; Barmby et al. 2000) have relied on correlations of spectroscopic metallicity and/or reddening-free parameters with intrinsic color. This procedure necessarily requires a calibration from the Galactic clusters and the assumption of similar extinction laws, but Barmby et al. (2000) showed that both of these steps were reasonable.

The first step in determining the extinction of the M31 GCs is to decide on a value for the foreground extinction. The H I maps of Burstein (1984) and the DIRBE/IRAS maps of Schlegel, Finkbeiner, & Davis (1998) agree that the Galactic reddening in the direction of M31 is $E(B - V) =$

0.08, corresponding to $A_V = 0.25$. In Barmby et al. (2000), we found that the average reddening of the M31 halo GCs is consistent with this value, although the individual reddening values had a large scatter. Since about half the halo clusters do not have reliable reddening values, and about 20% have no reddening determination at all, we choose to use a single value, the foreground reddening, for all the halo clusters. A few halo objects had well-determined reddening values that were higher than this, but adopting a single value for all objects simplifies comparison of our results with those of other authors.

Adopting a single extinction value for the M31 disk clusters is, of course, not reasonable. Fortunately, most of the disk objects in our GCLF sample (161/226) have reliable reddening values determined in Barmby et al. (2000). A few of the reliable values are actually below the foreground value, and we replaced them with the foreground value. Some of the objects without reliable reddening had a high value of $\sigma_{E(B-V)}$. We examined the values of $E(B-V)$ from individual colors for these objects, and found that removing one or two discrepant values usually yielded an acceptable error in the resulting reddening value. This left 42 objects without reddening values. For these objects we estimated the reddening by computing the average reddening of objects projected within $10'$, weighted by the inverse of the projected distance. This procedure is somewhat arbitrary, and may yield erroneous results if the ‘nearby’ clusters are at significantly different distances along the line of sight. A test of the technique on GCs with measured reddening values produced reassuring results: the average offset between measured and estimated reddening values was 0.00 ± 0.01 mag, although the scatter in the offset was large (0.19 mag). We compute extinction values from $E(B-V)$ using the curve for $R_V = 3.1$ given in Cardelli, Clayton, & Mathis (1989).

3.3. Completeness correction

While we do not have a quantitative estimate of the magnitude of completeness and contamination in our catalog as a whole, there are two effects for which we can correct. One effect is incompleteness caused by our magnitude limit. This is somewhat complicated because we use an observational (i.e. uncorrected for extinction) magnitude limit but we need to determine the completeness function in extinction-corrected magnitudes, where we measure the GCLF. For example, we believe our sample of all M31 clusters is complete to $V_{\text{lim}} = 18$, but this does not mean it is complete to $V_0 = 17.75 = 18 - A_V(\text{min})$. Heavily-extinguished clusters would have $V > 18$ but $V_0 < 17.75$. We compute the required completeness correction in V_0 bins as follows. First, we divide each bin into five smaller sub-bins. For each sub-bin, we use the observed distribution of extinction values to determine the fraction of the bin which could have been observed, i.e. for which $V_0 + A_V < V_{\text{lim}}$. This fraction is the completeness fraction, which we average over the sub-bins to determine the completeness for each bin. We use the same procedure to correct for the effects of the magnitude limit in V on data in other bandpasses (written generically as X_0). In this case both the color and extinction distributions are taken into account, and the objects which could have been observed have $X_0 + (V - X_0) = X_0 + (V - X_0)_0 + A_V < V_{\text{lim}}$. We compute individual

completeness functions for all of the different M31 GC samples discussed in this paper.

We performed Monte Carlo simulations to check that this correction procedure did not introduce a bias in the GCLF results. We generated V_0 GCLFs from Gaussian and t_5 (Secker 1992) distributions with $V_0 = 17.0$, $\sigma_g = 1.1$, $\sigma_t = 0.9$, $N_{gc} = 300$, parameters appropriate to the M31 GCLF. We applied to each object an extinction chosen randomly from the observed distribution, removed the objects with $V > V_{\text{lim}}$, generated the completeness function using the remaining objects, and measured the GCLF parameters of the sample. We corrected the GCLF parameters for the magnitude limit of each of the 200 trials using the method described in the following section. Over all trials, the averages of the peak location measure were 16.97 ± 0.01 for Gaussian and 17.04 ± 0.01 for the t_5 distribution; the average measures of dispersion were $\sigma_g = 1.10 \pm 0.01$, $\sigma_t = 0.92 \pm 0.01$. The uncertainties in the 200 individual measurements of peak location and dispersion (~ 0.18 and 0.13 mag, respectively) are large compared to the average difference between input (simulated) and output (measured) GCLF parameters, so we conclude that our completeness correction does not introduce a significant bias.

Another kind of incompleteness we correct for is missing photometry. We have V magnitudes for all of our objects, but observations in other filters are not always available. Estimating the photometric completeness in bands other than V is a simple procedure:

1. Set up a series of bins in magnitude X_0 .
2. Sort objects with known X_0 magnitude into the appropriate bin.
3. Estimate the X_0 magnitudes of the other objects as $V - (V - X_0)$, where $(V - X_0)$ is drawn at random from the probability distribution of the objects with X_0 , and sort them into the appropriate bins.
4. Add the bin totals from the previous two steps.
5. For each bin, the photometric completeness is (number of objects with measured X_0)/(total number of objects in bin).

The final completeness function is the average of 500 trials of steps 3–5, in order to average out the noise produced by drawing colors at random from the observed color distribution. The completeness function from missing photometry is multiplied by the completeness function for the magnitude limit to produce the final estimate of completeness in each bandpass.

We also checked the effects of errors in photometry and reddening on the GCLF results. Photometric uncertainties for the CCD and photoelectric photometry in our catalog are generally $\lesssim 0.05$ mag; uncertainties for photographic photometry (which is relatively uncommon in our catalog) are larger, perhaps 0.15 mag. These uncertainties are smaller than the errors in individual extinctions: in Barmby et al. (2000) we estimated uncertainties in $E(B - V)$ to be 0.05 – 0.10 mag, corresponding to A_V uncertainties of 0.16 – 0.31 mag. Using the same Monte Carlo simulations

described above, we added Gaussian errors (from distributions with zero mean and standard deviations from 0.15–0.50 mag) to every individual extinction in each of the 200 GCLFs. If an ‘extinction-with-error’ value fell below the foreground value of 0.25, the extinction was changed to the foreground value as in our observational procedure. We also added errors to the measured magnitudes, again drawn from Gaussian distributions with zero mean and dispersion increasing as $10^{0.2m}$ (the behavior expected from photon statistics).

Even large ($\sigma_{A_V} = 0.50$ mag) extinction errors did not change the average peak and dispersion measured for the GCLF ensemble by more than about 0.03 mag. Little change in the peak is expected, since the extinction errors have zero mean and even an error of 0.5 mag does not shift many observed magnitudes beyond the magnitude limit. The small effect of σ_{A_V} on the measured GCLF dispersion ($\sigma_g \approx 1.1$ mag) is explained by noting that the two dispersions combine in quadrature and, for large values of σ_{A_V} , the magnitude limit truncates the observed distribution width. Large magnitude errors ($\sigma_m \gtrsim 0.3$ at $V = 17$, much larger than our estimated uncertainties) biased the average GCLF peaks to brighter values but did not significantly affect the dispersions. These effects are not unexpected: large magnitude errors push more objects beyond the magnitude limit (resulting in a brighter peak) and the magnitude again limit truncates the observed distribution width. We conclude that extinction errors and magnitude uncertainties do not significantly affect our measurement of the GCLF parameters.

4. The GCLF

To compute the globular cluster luminosity functions, we used version 2.01 of the maximum-likelihood code described by SH93. This program estimates the maximum-likelihood values of the parameters $\hat{\Theta} = (\hat{m}^0, \hat{\sigma})$ by finding the maximum in the likelihood function

$$L(\Theta) = \log l(\Theta) = \sum_{i=1}^N \log[\phi(m_i)]. \quad (1)$$

The simultaneous distribution function $\phi(m)$ is evaluated for each of the N magnitude observations m_i :

$$\phi(m) = I(m)\gamma(m) \quad (2)$$

$I(m)$ is the completeness function and $\gamma(m)$ is the intrinsic GCLF — a Gaussian or t_5 distribution with center m^0 and dispersion σ . This is a simplified version of SH93’s $\phi(m)$; we set the number of background objects to zero as we do not have a quantitative estimate of the contamination rate. We also do not use the option to convolve the GCLF with the photometric error distribution: our photometry and extinction errors are not well-defined functions of magnitude, and trials using rough estimates of the error distributions showed that this did not significantly change the results. Uncertainties in the parameters are determined by computing $l(\Theta)$ over a grid in parameter space centered on the most probable parameter values. The resulting grid of likelihood values is normal-

ized to have a total probability of unity and collapsed along the parameter axes; the 1σ ranges for the parameter estimates are the ranges containing 0.68 of the total probability along each axis.

SH93 show that the results of their maximum likelihood procedure are biased by the existence of a magnitude cutoff. The brighter the limiting magnitude, the more the parameter estimates are biased toward brighter m^0 and lower σ . To correct for this effect, we use the results of their simulations, shown in their Figure 3.³ The equation used is:

$$\hat{m}^0 = m^0 + \delta(m_l - m^0) \quad (3)$$

where \hat{m}^0 is the estimated value of the turnover produced by the ML method, m^0 is the true, unbiased value, m_l is the limiting magnitude, and δ is the function plotted in the top panel of Figure 3 in SH93. We fit a fourth-order polynomial to δ , and use it to solve for m^0 given \hat{m}^0 and m_l . We fit a different polynomial $\tilde{\delta}$ to $\hat{\sigma} = \sigma + \tilde{\delta}(m_l - m^0)$ and compute σ directly after computing m^0 .

4.1. Results

We discuss the halo sample first, because most of the recent determinations of the M31 GCLF have been for this sample. Since the halo sample is close to complete, we can also estimate the GCLFs in other bandpasses without correcting for a V magnitude limit. Figure 2 and Table 2 show the GCLFs for the halo clusters in six bandpasses. The Gaussian and t_5 distributions give indistinguishable results for the location of the GCLF peak. The best-fit Gaussians have smaller values of the dispersion: the characteristic $\sigma_g \approx 1.05$ corresponds to $\sigma_t = 0.82$. This is not a serious concern; Secker (1997) notes that the theoretical correspondence between σ_g and σ_t ($\sigma_g = 1.29\sigma_t$) is seldom observed for the small number of objects used here. The t_5 form of the GCLF has smaller parameter uncertainties than the Gaussian form. This implies that the t_5 function is a better fit to the GCLFs than the Gaussian, and indeed a comparison of the maximum likelihood values shows this to be true in almost all cases. The superiority of the t_5 function over the Gaussian was first pointed out by Secker (1992), and confirmed by SH93. In the remainder of this paper, we consider only the t_5 estimates of the GCLF parameters. The sixth column of Table 2 shows the differences between the mean colors of the objects and the mean peak colors, measured relative to V . The differences are well within the uncertainties of the peak locations, as would be expected if the halo GCs have no correlation of color with magnitude. This means that, given sufficiently accurate estimates of the clusters' mean intrinsic colors (which requires an accurate determination of the reddening), the GCLF peak in one band can be used to estimate peak locations in others bands.

Next we compare our results to previously published M31 GCLFs, given in Table 3. We correct the values for the GCLF peak for our preferred extinction value, $A_V = 0.25$. Where the peak values

³We note what appears to be a misprint in SH93: in both Figure 3 and the text, $(m^0 - m_l)$ appears where $(m_l - m^0)$ is clearly implied.

were given as extinction-corrected absolute magnitudes M_V^0 , we used the corresponding apparent distance moduli μ_V to convert the values to V_0^0 . The relation used was

$$V_0^0 = M_V^0 + \mu_V - A_V' + \Delta A_V \quad (4)$$

where A_V' is the previous author’s assumed extinction and $\Delta A_V = A_V' - 0.25$. [Sharov & Lyutyi (1989) estimated extinction internal to M31 for each cluster, using $R_V = 2.65$. We could not correct these extinctions to our values because the individual magnitudes and extinctions were not given, but we did apply a correction for the foreground extinction.] Our results for the halo GCLF peak and dispersion, $V^0 = 16.84 \pm 0.11$, $\sigma_t = 0.93 \pm 0.13$, are consistent at the 1σ level with the results for the $R > 10$ kpc sample of Crampton et al. (1985), the halo sample of Secker (1992), and the ‘outer’ sample of Gnedin (1997). We find a brighter peak than Racine & Shara (1979); their photographic photometry may be suspect. Because the number of halo clusters is small, the composition of the sample can measurably change the derived GCLF parameters. If we drop the five ‘low-probability’ clusters mentioned in Section 3.1 from our sample, we recover the slightly brighter peak value reported by Secker (1992). We are aware of only one measurement of a non- V -band GCLF peak in M31: Sandage & Tammann (1995) average the B magnitudes of Secker’s halo sample to obtain $\langle B \rangle = 17.75 \pm 0.11$, which corresponds to $B_0^0 = 17.42 \pm 0.11$. This is again consistent with our result at the 1σ level.

We now turn to the other samples of M31 GCs. Here we consider only the V -band GCLF, as the photometric completeness in other bands is generally much poorer. We correct the GCLF peaks and dispersions for the magnitude cutoff at $V = 18$. The full and disk samples have similar GCLF peaks (16.70 ± 0.11 , 16.67 ± 0.16) and dispersions ($\sigma_t = 1.11 \pm 0.09$, 1.18 ± 0.12); this is unsurprising as the full sample is 77% disk clusters.⁴ We find a fainter GCLF peak for the GCS as a whole than do Crampton et al. (1985), Sharov & Lyutyi (1989), and Gnedin (1997) (considering here the ‘all clusters’ samples of Crampton et al. and Gnedin). There are several likely reasons for this: the older samples are less complete and have poorer photometry, and their corrections for incompleteness are either non-existent or do not account for the extinction effect discussed in Section 3.3.

Neither the full or disk samples has a GCLF peak significantly different from that of the halo, but the disk sample has a 2σ higher dispersion than the halo. This is in contrast to previous results: both Crampton et al. (1985) and Gnedin (1997) found the GCLF peak to be brighter and the GCLF dispersion lower for the inner (‘disk’) clusters. We suspected that the peak difference found by other groups was because they failed to correct for incompleteness due to extinction. To test this, we tried setting the completeness function to a step function with the step at $V_0 = 17.75$. The result was a much brighter disk peak, resulting in a difference of 0.6 mag between the halo

⁴The GCLF parameter uncertainties are smaller for the halo than for the disk sample, even though the disk has about 2.5 times as many objects. This is caused by extinction-induced incompleteness: when completeness is not corrected for, the uncertainties drop by $\sim 50\%$. In the halo sample, the uncertainties are close to the limit imposed by the small numbers: $\sigma_g/\sqrt{N} \approx 0.11$.

and disk GCLF peaks. The completeness correction thus has a large effect on the resulting GCLF, and the extinction cannot be ignored in a spiral galaxy like M31. We address the question of lower halo dispersion in Section 4.3.

Models of GCS evolution predict that low-mass clusters near the center of a galaxy are most susceptible to dynamical destruction. We suspected that our disk/halo division might be too crude to detect any radial GCLF differences. We followed the method of Gnedin (1997) in sorting the M31 clusters by projected distance from the center of M31 and dividing them into equal-sized groups. As Figure 3 shows, there is a definite trend for the GCLF peak to be fainter with increasing projected distance, although the GCLF dispersion does not show any obvious trend. The difference between the inner- and outer-most groups ranges from 0.44 to 0.56 (± 0.18) mag in V_0 , depending on the number of groups, with $\Delta m^0/\sigma(m^0) = 2.5 - 2.8$. The trend in the peak is largely due to the objects with $R \lesssim 3$ kpc. The disk is dominated by GCs with larger R_{gc} , which is why we see little difference between the disk and halo samples. This again underscores the importance of having a complete, uncontaminated sample of the GCs near the M31 nucleus.

Both Huchra, Brodie, & Kent (1991) and Barmby et al. (2000) found that the metal-rich clusters were more centrally concentrated. Could a difference between MR and MP GCLFs produce a radial GCLF difference? To disentangle the effects of age and metallicity, we divided our full sample by both metallicity and projected galactocentric distance. Since the radial GCLF variation is mostly due to the innermost clusters, we put the inner/outer dividing line at the galactocentric distance containing one-third of the clusters, $R \approx 3.8$ kpc = $19'$. The resulting GCLF parameters are in Table 4; the GCLFs and completeness functions are shown in Figure 4. The significant difference between GCLF parameters of MR and MP clusters in the outer two-thirds of M31 strongly implies that both metallicity (or some parameter related to it) and galactocentric distance affect the GCLF peak. To check that the effect we measured was not due to the details of sample division, we carried out 200 trials in which we divided the full sample in both metallicity and R_{gc} , with randomly chosen division points. While the differences between subsamples depended on the exact division point (as expected), the relative ordering of the GCLF peaks was always the same as that shown in Table 4.

The size of each parameter’s contribution to the GCLF peak can be estimated by writing the values as:

$$\begin{pmatrix} \text{MP}_i & \text{MR}_i \\ \text{MP}_o & \text{MR}_o \end{pmatrix} = \begin{pmatrix} 16.32 & 16.15 \\ 17.02 & 16.46 \end{pmatrix} = \begin{pmatrix} 16.42 & 16.06 \\ 16.92 & 16.56 \end{pmatrix} + \begin{pmatrix} -0.10 & 0.10 \\ 0.10 & -0.10 \end{pmatrix} \quad (5)$$

so 0.50 mag of GCLF variation is due to galactocentric distance, 0.36 mag to metallicity, and 0.10 to the interaction of the two. This is very similar to the average results from the 200 ‘random division point’ trials. The existence of the interaction term is not surprising, since we know that metallicity and galactocentric distance are correlated (e.g., see Figure 21 of Barmby et al. 2000).

Another way to quantify the GCLF variation is a multiple regression of V_0^0 on $[\text{Fe}/\text{H}]$ and projected galactocentric distance R_{gc} . We performed such a fit for the data in the first four rows of Table 4. Although using four points to define a plane is not statistically rigorous, it is a reasonable

way to estimate the size of the effects $[\text{Fe}/\text{H}]$ and R_{gc} have on the GCLF. (Defining the relation more rigorously will be difficult, since measuring GCLF parameters with reasonable precision requires sample sizes $N \gtrsim 50$ and the full M31 GC sample of 294 objects can only be divided into a few independent subsamples.) The regression equation is:

$$V_0^0 = 15.67 - 0.24[\text{Fe}/\text{H}] + 0.12R_{gc} \quad (6)$$

with $[\text{Fe}/\text{H}]$ in dex and R_{gc} in kpc. This equation predicts V_0^0 to within ≤ 0.15 mag for the last four samples in Table 4 (see Figure 5), where the clusters are separated on either metallicity or R_{gc} but not both. A multiple regression of V_0 on $[\text{Fe}/\text{H}]$ and R_{gc} for the individual cluster data (with no incompleteness correction) gives similar regression parameters, but the correlation is much poorer because of the luminosity dispersion. This is why we did not detect any correlation of luminosity with metallicity in Barmby et al. (2000), and why we believe that binning the clusters into samples, although arbitrary, is necessary.

The surprising result here is that the MR clusters are *brighter* than the MP clusters. For clusters of the same age, and average metallicities $[\text{Fe}/\text{H}] \sim -1.6$ and -0.6 , Ashman et al. (1995) predict that the MR clusters should be fainter in V by 0.29 mag. A difference in age between the two metallicity groups could be responsible, as younger clusters are expected to be brighter; we return to this point in the following section. The only systematic error we can conjecture which would cause overly bright magnitudes for the MR clusters is an overestimation of their extinction. However, this would also make the derived intrinsic colors of the MR clusters too blue, which seems unlikely given that the color-metallicity relations for Galactic and M31 clusters match well throughout their metallicity range (see Barmby et al. 2000).

Reports of large GCLF variations with either R_{gc} or metallicity are not common in the literature. Armandroff (1989) assigned Milky Way GCs to the disk or halo based on $[\text{Fe}/\text{H}]$ (with a dividing line at -0.80 dex) and found no difference in the luminosity functions of the two groups. Kavelaars & Hanes (1997) found no difference in GCLF peak magnitudes of the inner and outer halo clusters in the Milky Way and M31; Gnedin (1997) found a 0.47 mag difference between GCLF peaks of the same samples and claimed that the histogram-fitting method used by Kavelaars & Hanes was responsible for their failure to detect the difference. Gnedin (1997) also found a difference of 0.79 ± 0.12 mag in GCLF peak magnitudes between inner and outer GCs in M31. This difference is larger than the one we measure, but certainly compatible with it at the 1σ level. Selection effects in our M31 GC catalog are a possible cause of the differences between our results and those of previous authors; we consider this in the following section.

Most published GCLFs are actually for elliptical galaxies – M31 and the Milky Way are the only two spirals whose GCLFs are well-measured (but these two galaxies are often used, e.g. by Sandage & Tammann (1995), to define the GCLF peak absolute magnitude for use in distance measurement). In ellipticals where GCLFs have been determined separately for the red (MR) and blue (MP) GCs (e.g. Kundu et al. 1999; Puzia et al. 1999; Grillmair et al. 1999) the metal-poor clusters are typically found to be brighter (0.1–0.5 mag) in V , and fainter or similar in I , as

predicted by Ashman et al. (1995). Lee & Kim (2000) analyzed the same HST data as Puzia et al. (1999), but found that GCLF peaks of the red and blue clusters were indistinguishable in both V and I . Gnedin (1997) found a 0.24 ± 0.11 mag difference between the GCLF peaks of inner and outer clusters in M87, while Kundu et al. (1999) found no evidence for radial variation in the M87 GCLF and suggested that Gnedin did not correctly account for incompleteness. Puzia et al. (1999) found that only the red clusters in NGC 4472 show a difference between inner and outer GCLF peaks (0.27 ± 0.14 in V). Our results on the radial GCLF variation are not inconsistent with those of other authors, but the variation with metallicity or color has not been reported before. It is important to know whether the GCLF variation we measure is a unique feature of the M31 GCS, a common feature of spiral galaxies’ GCSs not shared by the Milky Way, or an artifact of the data and methods we used. A definitive answer to this question will require better data on the M31 clusters and their individual extinctions and information on the GCLF in other spirals.

4.2. Selection effects and the GCLF

Because M31 GC catalogs, including ours, suffer from both incompleteness and contamination, it is reasonable to ask how the catalog properties might affect the GCLF. Specifically, could variations in the degree of contamination and incompleteness with galactocentric distance be responsible for the radial GCLF variations we measured?

A small fraction of the objects in our cluster catalog are probably not M31 GCs. Of the 294 objects in our full sample, 178 (about 60%) have been confirmed as clusters by spectroscopy or high-resolution imaging. Most of the halo sample (73/86) is confirmed, and Figure 6a shows that the fraction of confirmed clusters is highest in the outer regions. The confirmed objects also tend to be brighter, as Figure 6b shows: this is not surprising since the largest spectroscopic survey (that of Huchra et al. 1991) was performed descending a magnitude-ordered list. We are not aware of any ‘false positives’ — objects whose confirmation as a GC was later shown to be incorrect — among M31 GC candidates, so any non-clusters must therefore be among the 116 unconfirmed objects. Since these objects are, on average, fainter than the confirmed clusters, dropping contaminating objects from the sample should make the resulting GCLFs brighter. A larger effect would be expected for the inner region, since it has more unconfirmed objects.

We tested this hypothesis using a Monte Carlo experiment. For the full sample and each of the subsamples listed in Table 4, we performed 200 trials in which we chose 34% of the unconfirmed clusters at random, dropped them from the sample, and computed the GCLF with the remaining objects. The 34% figure comes from the Battistini et al. (1987) classification of these objects and Racine’s (1991) estimate of the actual cluster fractions in each class. Table 5 shows the average of the GCLF parameters over all 200 trials. Compared to the full samples (Table 4), the GCLFs found for the ‘decontaminated’ samples had brighter average peaks and almost identical dispersions; this was expected because most of the unconfirmed clusters are faint. The change caused by decontamination was larger for the inner and metal-rich clusters; again, this was expected because these clusters

are less likely to be confirmed. Table 6 shows that decontaminating the cluster catalog actually increases the GCLF peak and dispersion differences between different samples. We conclude that contamination of the GCLF sample by non-clusters cannot be responsible for the GCLF differences we measure.

A first attempt at estimating the catalog incompleteness can be made using the work of Mochejska et al. (1998). They searched for globular clusters in four fields on the eastern side of the M31 disk ($R_{gc} \sim 20\text{--}40'$) with a total area of 440.7 square arcmin. Mochejska et al. discovered 67 new GC candidates in this region, but considered all except five to be low-probability candidates. Two of the five good candidates had $V < 18$ and three had $V > 18.5$. The area of the the M31 disk (the large ellipse in Figure 1) is 1.14×10^4 square arcmin, so can we scale the Mochejska et al. (1998) result by area to estimate that our catalog could be missing as many as 50 clusters with $V < 18$. We do not have any information on the magnitude distribution of the possible missing clusters, other than the fact that virtually all of Mochejska et al.’s new cluster candidates have $V \gtrsim 17.5$. If our catalog were truly missing 50 objects, it would be about 83% complete. Because this value is a large extrapolation from very few data points, it can only be considered a rough estimate of our catalog’s completeness, and it yields no information on completeness variation with magnitude or galactocentric distance.

An incompleteness estimate based on the work of Mochejska et al. (1998) is suitable for the outskirts of M31, but not for the crowded inner region. To estimate the number of missing GCs and contaminating objects in this regions, we used data in the HST Archive to search for new and previously known M31 GCs; the details of this effort will be described in a subsequent paper (Barmby & Huchra, in preparation). Briefly, we examined all 79 WFPC2 fields with $R_{gc} \leq 30'$ imaged with broadband optical filters (F300W to F814W) and with exposure times ≥ 100 s. We chose $R_{gc} = 30'$ as the outer limit because the fractional area of M31 covered by HST fields is only 5% at this distance and the chances of finding globular clusters in more distant fields are small. Working independently, two of us (PB and JH) visually searched each image for globular clusters. The searches were conducted ‘blind’, i.e., with no reference to the positions of known M31 GCs. To estimate our cluster detection efficiency, we inserted ‘artificial’ globular clusters, made by randomly rotating and re-scaling HST images of known M31 globulars, into some of the images. Our overall success rate for detection of the artificial clusters over the magnitude range $14 < V < 22$ was 80%; for objects with $V < 18$, our primary concern for this work, our success rate was 96%. We conclude that we should have detected essentially all true M31 GCs with $V < 18$ in the HST images.

Our final list of cluster candidates contains 62 objects. 40 of these are previously-discovered objects appearing in our catalog (Barmby et al. 2000) of plausible cluster and candidates, 9 are previously-discovered objects not in our catalog because they had been classified as ‘low-probability’ candidates, and 13 objects are newly-discovered cluster candidates. We estimated V magnitudes for the new candidates from the HST images, using the transformations given in Holtzman et al. (1995). Figure 7 shows the distribution of the HST cluster candidates in V and R_{gc} . Only about half of the non-cataloged objects are unquestionably globular clusters, so we mark ‘good’ and ‘marginal’

candidates with different symbols. Most of the newly-discovered candidates are either faint objects at large galactocentric distances, or bright objects very close to the galaxy center. The discovery of bright new cluster candidates having $R_{gc} \leq 5'$ shows that incompleteness is substantial in the region, and validates our decision to exclude it from GCLF computations.

The important question here is whether there is a difference in catalog completeness between inner and outer clusters with $V < 18$. In the inner region there were 20 good GC candidates with $V < 18$; 17 of these objects were in our catalog, so its completeness is 85%. In the outer region there were 8 good GC candidates with $V < 18$; only one of these objects was not in our catalog, so the completeness is 88%. Although the numbers are small because the covering fraction of the HST images on the sky is only 10–20%, there is no evidence that the inner sample of clusters is substantially less complete than the outer one. The new cluster candidates in both regions have similar magnitudes, $V \sim 17.7$, indicating that the magnitude limit of the existing catalogs does not change drastically with R_{gc} .

To the best of our ability to model them, the selection effects of incompleteness and contamination in the M31 cluster sample are not responsible for the GCLF variations which we measure. The M31 GC catalog can certainly be improved, and our conclusions would be strengthened if the same GCLF differences were measured in less-contaminated samples with better-understood and spatially uniform completeness. However, analysis of the GCLF does not require a perfect catalog — something which does not exist even for the Milky Way GCs. As a final comment on catalog incompleteness, we speculate on the possibility that there exists a heavily-obscured population of GCs in M31. If such objects exist and are fainter than the known population *and* preferentially located near the center of M31 or metal-rich, then the brighter peaks found for the metal-rich and inner clusters might be an artifact of incompleteness. There is presently no evidence for a population of heavily-extinguished GCs in M31, so we believe our GCLF results to be valid, and consider their implications in the following section.

4.3. Implications for GCS destruction and formation models

Variation of the GCLF with R_{gc} is a key prediction of GCS evolution models. The shorter destruction timescales for clusters near the center of a galaxy potential may lead to a mass difference, and hence a GCLF difference, between ‘inner’ and ‘outer’ GCs in a galaxy. Several authors have predicted differences between the inner and outer GCLFs for Milky Way clusters. The dividing line between inner and outer varies from 5–10 kpc, and the size of the predicted difference in the GCLF peaks ranges from essentially zero (Vesperini 1998) to 1.4 magnitudes (Baumgardt 1997). Vesperini (1998) finds that there is a particular initial GCMF for which the balance between cluster disruption and mass evolution of the surviving clusters keeps the shape and initial parameters of the mass function unchanged. The only prediction made specifically for the M31 GCS is that of

Ostriker & Gnedin (1997). For an inner/outer split at $R = 27' = 5.5$ kpc,⁵ they predict a peak location difference of 0.49 ± 0.18 . Our results on the GCLF peak are in excellent agreement with this prediction. For two populations of the same age and metallicity, a magnitude difference of 0.5 corresponds to a mass ratio of $10^{0.2} = 1.58$. For populations with the same age and metallicities differing by 1 dex, a magnitude difference of 0.35 in V implies a mass ratio of 1.87; the larger mass ratio is due to the increase of mass-to-light ratio with metallicity.

Ostriker & Gnedin (1997) predict that destruction of low-mass inner clusters results in a (Gaussian) GCLF dispersion for the inner clusters 0.17 ± 0.12 mag lower than that of the outer clusters. Vesperini (1998) also predicts a lower inner GCLF dispersion for most initial conditions. We do not measure a lower GCLF dispersion for the inner clusters: if anything, the dispersion seems to decrease, not increase, with projected distance. While photometric and extinction errors are probably larger for the inner clusters, we showed in Section 3.3 that only very large errors strongly bias the GCLF parameters. The completeness limit is brighter for the inner clusters; again, this should not affect the GCLF parameters since we correct for the resulting bias. We are unable to devise any other systematic effects which might lead to erroneous measurements of the GCLF dispersion. A larger age spread in the inner clusters might mask a decrease in GCLF dispersion. If such an age spread existed in M31, it would be in contrast to the Galactic GCS, where the age spread is larger for the outer clusters (Chaboyer, Demarque, & Sarajedini 1996). It is also possible that the inner clusters had a log-normal initial GCMF with parameters that resulted in evolution in mean mass but not in dispersion (see Vesperini 1998). Since the theoretically predicted dispersion differences are small compared to the peak location differences, we do not consider our failure to detect such differences a serious problem for either our method or the theoretical models.

Key assumptions made when calculating the effects of dynamical destruction on the GCLF are that the initial age and mass distributions of the GCs are not functions of R_{gc} , and that metallicity effects are not important. These assumptions may not be correct. Barmby & Huchra (2000) found evidence that the metal-rich clusters in M31 and the Milky Way were younger than the metal-poor clusters; Rosenberg et al. (1999) found similar results from the color-magnitude diagrams for a sample of Milky Way clusters. If age differences do exist, they should affect the GCLF. To estimate the size of the age difference, we examined the predictions of V -band luminosity in the models of Bruzual & Charlot (1996), Kurth, Fritze-von Alvensleben, & Fricke (1999), and Worthey (1996). We computed the age differences implied by $\Delta V = 0.35$ mag, with (fainter, brighter) populations at $[\text{Fe}/\text{H}] = (-1.63, -0.63)$ (Bruzual & Charlot 1996; Kurth et al. 1999) or $(-1.50, -0.50)$ (Worthey 1996). Worthey’s models cover only the age range from 8–16 Gyr at these low metallicities, and the only age pair with the required ΔV is $\text{age}_{\text{MR}} = 8$ Gyr, $\text{age}_{\text{MP}} = 16$ Gyr. For the other two sets of models, which cover the age range 1–16 Gyr, several age pairs reproduce the GCLF peak difference. In each case the MR clusters are about half as old as the MP clusters. Explaining the

⁵It is unclear whether this value is a projected or true 3-D distance from the center of M31; we assume it to be a projected distance.

GCLF difference of outer and inner clusters as an age difference is also possible. For populations of the same metallicity (the median $[\text{Fe}/\text{H}]$ values of the inner and outer clusters are not very different at -1.27 and -1.41), a 0.5 mag difference in V corresponds to the brighter clusters being 55% as old as the fainter clusters.

If the two sets of clusters have the same stellar initial mass function (IMF), the effect of IMF on the derived age differences is fairly small. For a Scalo (1986) or Miller & Scalo (1979) IMF instead of Salpeter (1955), $\Delta V = 0.35$ at different metallicities makes the MR clusters about 55% as old as the MP clusters, and $\Delta V = 0.5$ at the same metallicity makes the bright clusters 60% as old as the fainter ones. However, if the two sets of clusters had *different* IMFs, this could produce a large difference in the average V magnitudes. All three models predict that Scalo-IMF populations should be brighter than Salpeter-IMF populations of the same age and mass, by $0.6 - 1.0$ mag in V for ages > 8 Gyr. A difference in IMF with metallicity would still require explanation, however; at least for Galactic GCs, De Marchi & Paresce (1999) find no evidence of IMF variation.

Independent constraints on cluster ages and IMFs are needed in order for GCLF variations to be used in the study of GCMF evolution. If different populations start with the same GCMF, differing dynamical evolution could lead to mass differences and explain the observed GCLF differences. However, combinations of age, metallicity and IMF differences could also reproduce the observations. With only one observable it is not possible to constrain all of the cluster parameters. Measuring the GCLF variations in the K -band, which is less sensitive to age and more sensitive to metallicity (the mass-to-light ratio in K is expected to decrease with metallicity, rather than increase as it does in V ; Worthey 1994) would be helpful in disentangling the two effects. Unfortunately, our catalog lacks near-IR photometry for many clusters in the disk, so it is not possible to accurately measure the near-IR GCLF for the inner clusters.

Examining the measured GCLF parameters leads to several important conclusions. The fact that metal-rich clusters are, on average, brighter than metal-poor clusters implies that there must be some mass, age, or IMF difference between the two groups. We consider here the extreme possibilities for age and mass differences that could reproduce this effect (we neglect possible IMF differences, since these seem the least likely). Either (1) the MR clusters are younger by $\sim 50\%$, or (2) the MR clusters are more massive by a factor of ~ 1.9 . The fact that inner MP clusters are brighter than outer MP clusters means that there is also a GCLF variation with R_{gc} . Again, the two extreme possibilities are: (3) the inner clusters are younger by $\sim 45\%$, or (4) the inner clusters are more massive by a factor of ~ 1.6 . Each of these possibilities has important implications for the understanding of GCS and galaxy formation and evolution; we examine each in turn, drawing on the review given by Kissler-Patig (2000).

1) If the MR clusters are younger than the MP clusters, an age-metallicity relation exists in the M31 GCS. Such a relation has long been suspected for the Galactic clusters, although it has not been demonstrated conclusively (see Sarajedini, Chaboyer, & Demarque 1997). Lee & Kim (2000) and Kundu et al. (1999) compared their GCLF measurements in NGC 4472 and

M87, respectively, to population synthesis models. Both found that, in addition to the metallicity effect, younger ages for the metal-rich clusters were required to account for the observed GCLF peak differences. A relation between age and metallicity is consistent with several scenarios for the formation of globular cluster systems. These include the merger scenario of Ashman & Zepf (1992), the in situ/two-phase scenario of Forbes, Brodie, & Grillmair (1997), and the pre-galactic scenario of Kissler-Patig (1997) (see also Peebles & Dicke 1968). Fitting young MR GCs in M31 into the merger scenario would require some modifications. The scenario attempts to account for the presence of multiple populations of GCs in *elliptical* galaxies by postulating that the MR clusters form when star formation is induced in the spiral/spiral merger which produces the elliptical. M31 would thus have to be a merger product itself. While there is little evidence that M31 has had a recent major merger, perhaps the ‘minor merger’ of a satellite galaxy with M31 could have excited star formation in the M31 disk (Hernquist & Mihos 1995), generating a population of younger GCs.

Forbes, Brodie, & Grillmair (1997) suggested that the two populations of GCs in ellipticals formed in two distinct phases separated by several Gyr, with the disk GCs in spirals representing a third collapse phase. The pre-galactic scenario also has two phases, but the difference is that the MP clusters are unrelated to the final galaxy. Either scenario is compatible with our results, although neither specifically predicts the large age difference we estimate or the relative number of MR and MP clusters. It is interesting that all three scenarios were devised to explain the multiple GC populations of ellipticals, but there is, so far, little evidence for any age-metallicity relation in the GCs of such galaxies. Cohen, Blakeslee, & Ryzhov (1998) found that their samples of MR and MP GCs in M87 are coeval and old (although they suggested that there may be a problem with their model calibration). Puzia et al. (1999) and Kissler-Patig et al. (1998) found similar results for NGC 4472 and NGC 1399, respectively.

2) Is the mass of M31 GCs somehow related to their metallicity? Massive clusters could have their metallicity increased by self-enrichment, and self-enriched GCs must be massive enough to survive disruption by supernova explosions. Morgan & Lake (1989) give a minimum mass for surviving GCs of $10^{4.6} M_{\odot}$, low enough to include almost all Galactic and M31 GCs. They state that “it is difficult to ‘predict’ any trend of metallicity with mass without extra information on the IMF”, but it seems logical that more massive clusters would generate a larger first generation of stars and hence have more enrichment. If self-enrichment occurred in Galactic GCs, it had to be rapid enough to produce the chemical homogeneity observed in most clusters (e.g. Suntzeff 1993). Parmentier et al. (1999) claim that, contrary to previous conclusions, the formation time for the second generation of stars is longer than the mixing timescale; if true, this means that self-enrichment (and a mass-metallicity relation) a realistic possibility. Instead of larger masses causing higher metallicity, could higher-metallicity gas induce the formation of more massive GCs? If metallicity is important in GC formation, the opposite seems more likely to be true. In models relying on a cooling condition (e.g. Murray & Lin 1992), MR clusters are predicted to be less massive (for the same IMF) because cooling is more efficient in high-metallicity clouds. An age-metallicity relation with a small mass-metallicity contribution from self-enrichment is our preferred scenario

for explaining the GCLF differences between MR and MP GCs in M31.

3) The possible explanations for younger inner clusters are similar to those for younger metal-rich clusters. The inner clusters could ‘naturally’ have formed much later than the outer clusters (during the end of the galaxy collapse phase?), or perhaps some external event caused the formation of inner GCs much later than the bulk of the population. Another possibility is that the inner clusters were accreted along with dwarf galaxies cannibalized by M31, although there is no obvious reason why dwarf galaxy GCs should be younger than those in larger galaxies. All of these scenarios are rather *ad hoc* and none are obviously related to theoretical ideas for globular cluster system formation. We do not consider any to be well-supported.

4) Globular cluster mass and galactocentric distance might be causally connected in either direction. Low-mass clusters are thought to be more easily destroyed near the galaxy center, leading to a larger average mass. This is one of the major predictions of models of GC destruction. Although model predictions vary widely, at least some models (e.g. Ostriker & Gnedin 1997) predict values for the GCLF difference close to what we observe. We do not measure the model-predicted difference in GCLF dispersion, but this may not be a serious problem. Could conditions near the galaxy center affect the average GC mass at formation? In the Murray & Lin (1992) GC formation scenario, GC mass is expected to *increase* with galactocentric distance, and we are aware of no models which explicitly predict a decrease in mean GC mass with distance. GC destruction by dynamical effects in the inner part of M31 is our preferred scenario for explaining the GCLF differences between inner and outer GCs in M31.

5. Conclusions

We have calculated the first *URJK* GCLFs for M31 halo globular clusters, and find that the GCLF peak colors are consistent with the average cluster colors. Our parameters for the *V*- and *B*-band halo GCLFs are consistent with those of other groups. We find no significant differences between the disk and halo GCLF peaks, although the disk has a lower dispersion. A difference in GCLF peak at the 2σ level occurs when we consider the inner and outer-most groups, as determined by projected galactocentric distance. This difference is consistent with that predicted by Ostriker & Gnedin (1997) for M31; however, we do not detect the predicted difference in GCLF dispersion. We separate the M31 clusters by metallicity and find that the metal-rich clusters have a brighter GCLF peak than the metal-poor clusters, even when the difference in R_{gc} is taken into account. Modeling of the catalog selection effects suggests that these effects are not responsible for the measured GCLF differences. However, an M31 GC catalog with well-understood and spatially uniform completeness and contamination is required in order to definitively confirm our results. Such a catalog might be produced by a near-IR, high spatial resolution survey of M31. We consider the implications of the GCLF differences for models of globular cluster and GCS formation, and conclude that younger ages for metal-rich clusters plus dynamical destruction of inner clusters are the most likely causes of the observed GCLF variations.

We thank the referee for incisive comments, G. Smith and L. Schroder for help with the Lick observations, and J. Secker for making his maximum-likelihood GCLF code available. We thank the staffs of Whipple and Lick Observatories for productive observing runs and patient post-observing support. This research was supported by the Smithsonian Institution, Faculty Research Funds from the University of California, Santa Cruz, and NSF grant AST-990732.

REFERENCES

- Armandroff, T. E. 1989, *AJ*, 97, 375
- Ashman, K. A. & Zepf, S. E. 1992, *ApJ*, 384, 50
- Ashman, K. M., Conti, A., & Zepf, S. E. 1995, *AJ*, 110, 1164
- Aurière, M., Coupinot, G., & Hecquet, J. 1992, *A&A*, 256, 95
- Barmby, P. & Huchra, J. P. 2000, *ApJ*, 531, L29
- Barmby, P., Huchra, J. P., Brodie, J. P., Forbes, D. A., Schroder, L. L., & Grillmair, C. J. 2000, *AJ*, 119, 727
- Battistini, P. L., Bònoli, F., Braccesi, A., Federici, L., Fusi Pecci, F., Marano, B., & Börngren, F. 1987, *A&AS*, 67, 447
- Battistini, P. L., Bònoli, F., Casavecchi, M., Ciotti, L., Federici, L., & Fusi Pecci, F. 1993, *A&A*, 272, 77
- Baumgardt, H. 1997, *A&A*, 330, 480
- Blakeslee, J. P. & Tonry, J. L. 1996, *ApJ*, 465, L19
- Bruzual, G. & Charlot, S. 1996, version of models reported in Leitherer et al. 1996, *PASP*, 108, 996
- Burstein, D. & Heiles, C. 1984, *ApJS*, 54, 33
- Cardelli, J. A., Clayton, G. C., & Mathis, J. S. 1989, *ApJ*, 345, 245
- Chaboyer, B., Demarque, P., & Sarajedini, A. 1996, *ApJ*, 459, 558
- Cohen, J. G., Blakeslee, J. P., & Ryzhov, A. 1998, *ApJ*, 496, 808
- Crampton, D., Cowley, A. P., Schade, D., & Chayer, P. 1985, *ApJ*, 288, 494
- De Marchi, G. & Paresce, F. 1999, in *American Astronomical Society Meeting*, Vol. 195, 312
- Dubath, P. & Grillmair, C. J. 1997, *A&A*, 321, 379

- Durrell, P. R., Harris, W. E., Geisler, D., & Pudritz, R. E. 1996, *AJ*, 112, 972
- Elias, J. H., Frogel, J. A., Matthews, K., & Neugebauer, G. 1982, *AJ*, 87, 1029
- Ferrarese, L. et al. 2000, *ApJ*, 529, 745
- Forbes, D. A., Brodie, J. P., & Grillmair, C. J. 1997, *AJ*, 113, 1652
- Forbes, D. A., Brodie, J. P., & Huchra, J. P. 1996, *AJ*, 112, 2448
- Gnedin, O. 1997, *ApJ*, 487, 663
- Grillmair, C. J., Forbes, D. A., Brodie, J. P., & Elson, R. A. W. 1999, *AJ*, 117, 167
- Harris, W. H. 1988, in *ASP Conf. Ser 4: The Extragalactic Distance Scale*, ed. C. Pritchett & S. van den Bergh (San Francisco: ASP), 231
- Harris, W. H. 2000, in *Saas-Fee Advanced Course on Star Clusters*, ed. ?? (New York: Springer-Verlag), 1
- Hernquist, L. & Mihos, J. C. 1995, *ApJ*, 448, 41
- Holtzman, J. A., Burrows, C. J., Casertano, S., Hester, J. J., Trauger, J. T., Watson, A. M., & Worthey, G. 1995, *PASP*, 107, 1065+
- Huchra, J. P., Brodie, J. P., & Kent, S. M. 1991, *ApJ*, 370, 495
- Kavelaars, J. J. & Hanes, D. A. 1997, *MNRAS*, 285, L31
- Kissler-Patig, M. 1997, PhD thesis, Sternwarte Bonn
- Kissler-Patig, M. 2000, astro-ph/0002070
- Kissler-Patig, M., Brodie, J. P., Schroder, L. L., Forbes, D. A., Grillmair, C. J., & Huchra, J. P. 1998, *AJ*, 115, 105
- Kundu, A., Whitmore, B. C., Sparks, W. B., Macchetto, F. D., Zepf, S. E., & Ashman, K. M. 1999, *ApJ*, 513, 733
- Kurth, O. M., Fritze-von Alvensleben, U., & Fricke, K. J. 1999, *A&AS*, 138, 19
- Lee, M. G. & Kim, E. 2000, *AJ*, 120, 260
- McLean, I. S. et al. 1994, in *Instrumentation in Astronomy VIII*, ed. D. Crawford (Bellingham: SPIE), 457
- Miller, G. E. & Scalo, J. M. 1979, *ApJS*, 41, 513
- Mochejska, B. J., Kaluzny, J., Krockenberger, M., Sasselov, D. D., & Stanek, K. Z. 1998, *Acta Astronomica*, 48, 455

- Morgan, S. & Lake, G. 1989, *ApJ*, 339, 171
- Mostek, N., Taft, A., Elias, J., & Geisler, D. 1999, in *American Astronomical Society Meeting*, Vol. 195, 310
- Murray, S. D. & Lin, D. N. C. 1992, *ApJ*, 400, 265
- Okazaki, T. & Tosa, M. 1995, *MNRAS*, 274, 48
- Ostriker, J. P. & Gnedin, O. 1997, *ApJ*, 487, 667
- Parmentier, G., Jehin, E., Magain, P., Neuforge, C., Noels, A., & Thoul, A. A. 1999, *A&A*, 352, 138
- Peebles, P. J. E. & Dicke, R. H. 1968, *ApJ*, 154, 891
- Persson, S. E., Murphy, D. C., Krzeminski, W., Roth, M., & Rieke, M. J. 1998, *AJ*, 116, 2475
- Puzia, T., Kissler-Patig, M., Brodie, J. P., & Huchra, J. P. 1999, *AJ*, 118, 2734
- Racine, R. 1991, *AJ*, 101, 865
- Racine, R. & Harris, W. E. 1992, *AJ*, 104, 1068
- Racine, R. & Shara, M. A. 1979, *AJ*, 84, 1694
- Reed, L. G., Harris, G. L. H., & Harris, W. E. 1992, *AJ*, 103, 824
- Reed, L. G., Harris, G. L. H., & Harris, W. E. 1994, *AJ*, 107, 555
- Rosenberg, A., Saviane, I., Piotto, G., & Aparicio, A. 1999, *AJ*, 118, 2306
- Salpeter, E. E. 1955, *ApJ*, 121, 161
- Sandage, A. & Tammann, G. A. 1995, *ApJ*, 446, 1
- Sarajedini, A., Chaboyer, B., & Demarque, P. 1997, *PASP*, 109, 1321
- Scalo, J. M. 1986, *Fund. Cosmic Phys.*, 11, 1
- Schlegel, D. J., Finkbeiner, D. P., & Davis, M. 1998, *ApJ*, 500, 525
- Secker, J. 1992, *AJ*, 104, 1472
- Secker, J. 1997, Documentation for version 2.01 of MAXIMUM.
- Secker, J. & Harris, W. E. 1993, *AJ*, 105, 1358
- Sharov, A. S. & Lyutyi, V. M. 1989, *AZh*, 66, 241

- Suntzeff, N. 1993, in *The Globular Cluster-Galaxy Connection*, ed. G. H. Smith & J. P. Brodie (San Francisco: ASP), 167
- Tollestrup, E. V. & Willner, S. P. 1998, *SPIE*, 3354, 502
- van den Bergh, S. 1985, *ApJ*, 297, 361
- Vesperini, E. 1998, *MNRAS*, 299, 1019
- Vetešnik, M. 1962, *Bull. Astron. Inst. Czech.*, 13, 218
- Whitmore, B. C. 1997, in *StScI Symposium Series 10: The Extragalactic Distance Scale*, ed. M. Livio, M. Donahue, & N. Panagia (Cambridge: Cambridge University Press), 254
- Wirth, A., Smarr, L. L., & Bruno, T. L. 1985, *ApJ*, 290, 140
- Worthey, G. 1994, *ApJS*, 95, 107
- Worthey, G. 1996, version of models reported in Leitherer et al. 1996, *PASP*, 108, 996
- Zepf, S. E., Ashman, K. M., & Geisler, D. 1995, *ApJ*, 443, 570

Table 1. New infrared photometry for M31 GCs

name	J	H	K
005-052	14.14(1)	13.78(2)	13.54(3)
150D	15.72(1)	15.17(1)	15.16(3)
167D	16.33(2)	15.69(2)	15.57(6)
196-246	15.37(1)	14.73(2)	14.60(3)
208-259	15.39(4)	14.71(4)	14.54(6)
232-286	14.05(1)	13.52(1)	13.34(2)
236-298	15.67(2)	14.99(2)	15.05(5)
242D	16.47(3)	16.32(5)	16.09(8)
316-040	15.36(4)
320-000	15.44(2)	...	14.15(3)
328-054	15.82(9)
329-000	15.94(3)	...	14.84(6)
330-056	15.84(7)
331-057	15.92(9)	...	14.89(12)
333-000	16.36(10)
336-067	16.14(2)	15.78(3)	15.65(7)
344D	15.39(7)
384-319	13.87(1)	13.14(1)	12.91(1)
399-342	15.69(2)	15.14(2)	15.07(4)
423-000	16.10(2)	15.48(2)	15.66(3)
450-000	16.65(5)	...	15.69(11)
457-097	15.38(2)	14.79(2)	14.79(3)
461-131	15.43(1)	14.78(1)	14.68(3)
469-220	15.92(2)	15.42(3)	14.92(4)
472-D064	13.46(1)	12.84(1)	12.63(2)
BA11	15.98(2)	15.65(3)	15.19(4)
DAO054	15.94(2)	...	14.90(4)
DAO055	17.02(7)
DAO094	15.88(3)	...	14.84(5)
DAO104	16.86(5)	...	15.82(11)

Objects with previous photometry

024-082	14.77(1)	14.13(1)	13.99(1)
027-087	13.85(1)	13.20(2)	13.13(2)

Table 1—Continued

name	J	H	K
042-104	13.21(1)	12.44(1)	12.28(1)
068-130	13.67(1)	12.86(1)	12.67(1)
082-144	12.43(1)	11.73(1)	11.44(1)
217-269	14.47(2)	13.82(2)	13.66(3)
298-021	14.97(1)	14.44(1)	14.39(3)
317-041	15.05(1)	14.62(2)	14.54(3)

Note. — Objects with H -band measurements were observed at Lick; others were observed at FLWO. Bracketed numbers are measurement uncertainties in hundredths of a magnitude.

Table 2. M31 Halo GCLF

bandpass	m_g^0	σ_g	m_t^0	σ_t	Δ_t	N
U_0	17.68 ± 0.21	1.05 ± 0.15	17.65 ± 0.13	0.87 ± 0.14	0.01	74
B_0	17.61 ± 0.21	1.12 ± 0.17	17.57 ± 0.14	0.95 ± 0.16	0.07	80
V_0	16.81 ± 0.13	1.06 ± 0.10	16.84 ± 0.11	0.93 ± 0.13	...	86
R_0	16.42 ± 0.19	1.10 ± 0.14	16.40 ± 0.14	0.95 ± 0.14	0.05	68
J_0	15.26 ± 0.20	1.08 ± 0.14	15.26 ± 0.14	0.98 ± 0.16	0.09	73
K_0	14.39 ± 0.20	0.97 ± 0.15	14.45 ± 0.18	0.89 ± 0.15	0.04	67

Note. — $\Delta = \overline{(V - X)}_0 - (V_0^0 - X_0^0)$ is the difference between the mean object color and the peak color. The superscript in V_0^0 refers to the GCLF peak, while the subscript refers to the extinction correction (Harris 1988).

Table 3. M31 V-band GCLF parameters

sample	V^0	σ (Gaussian)	N^a	Ext. correction ^b	Ref.
halo	16.54 ± 0.12	1.13	86	fg	(1)
all	16.95	1.2	188	fg	(2)
all	16.5	1.2	408	^c	(3)
$R < 10$ kpc	16.2	1.5	265	^c	(3)
$R > 10$ kpc	17.0	1.8	143	^c	(3)
all	16.13 ± 0.08	1.16 ± 0.08	294	M31+fg	(4)
halo	16.75 ± 0.11	1.10 ± 0.11	82	fg	(5)
halo	16.75 ± 0.15	1.10 ± 0.11	82	fg	(6)
halo	16.75 ± 0.15	...	81	fg	(7)
halo	17.20 ± 0.08	0.76 ± 0.05	161	fg	(8)
inner halo	17.05 ± 0.10	0.57 ± 0.10	64	fg	(8)
outer halo	17.04 ± 0.17	0.94 ± 0.13	97	fg	(8)
all	16.27 ± 0.06	0.86 ± 0.04	164	^c	(9)
inner	15.92 ± 0.08	0.70 ± 0.05	82	^c	(9)
outer	16.71 ± 0.09	0.96 ± 0.08	82	^c	(9)

^a N is the number of objects used in the GCLF measurement, not an estimate of the total number of GCs N_{gc} .

^b‘fg’ indicates correction for foreground extinction of $A_V = 0.25$ mag

^cPaper text implies that these values are corrected for extinction, but method not clearly described.

References. — (1) Racine & Shara (1979); (2) van den Bergh (1985); (3) Crampton et al. (1985); (4) Sharov & Lyutyi (1989); (5) Secker (1992); (6) Racine & Harris (1992); (7) Reed et al. (1994); (8) Kavelaars & Hanes (1997); (9) Gnedin (1997)

Table 4. GCLF for different samples of M31 GCs

Sample	m_t^0	σ_t	[Fe/H]	R_{gc} (kpc)	N
MP inner	16.32 ± 0.21	1.00 ± 0.17	-1.51	2.6	60
MP outer	17.02 ± 0.22	1.08 ± 0.13	-1.59	8.2	131
MR inner	16.15 ± 0.58	1.51 ± 0.32	-0.59	2.6	25
MR outer	16.46 ± 0.23	0.93 ± 0.18	-0.65	5.8	50
MP	16.84 ± 0.16	1.09 ± 0.11	-1.57	5.5	191
MR	16.43 ± 0.27	1.11 ± 0.19	-0.61	5.2	75
inner	16.37 ± 0.21	1.12 ± 0.17	-1.27	2.5	98
outer	16.80 ± 0.14	1.05 ± 0.10	-1.41	7.4	196

Note. — [Fe/H] and R_{gc} are median values.

Table 5. Average GCLF parameters for de-contaminated samples of M31 GCs

Sample	m_t^0	σ_t
MP inner	16.17	0.92
MP outer	17.00	1.12
MR inner	15.91	1.33
MR outer	16.35	0.93
MP	16.80	1.13
MR	16.28	1.12
inner	16.18	1.08
outer	16.74	1.07

Note. — Uncertainties in the parameter values from the 200 individual trials are comparable to those given in Table 4. Statistical uncertainties in the averages are much smaller, typically 0.05 mag.

Table 6. GCLF differences for full and de-contaminated samples of M31 GCs

Samples	Full samples		Decontaminated	
	Δm_t^0	$\Delta \sigma_t$	Δm_t^0	$\Delta \sigma_t$
outer–inner	0.43	–0.07	0.56	–0.01
MP–MR	0.39	–0.02	0.52	0.01
MP outer–MP inner	0.70	0.08	0.83	0.20
MR outer–MR inner	0.31	–0.58	0.44	–0.40
MP outer–MR outer	0.56	0.15	0.65	0.19
MP inner–MR inner	0.17	–0.51	0.26	–0.41

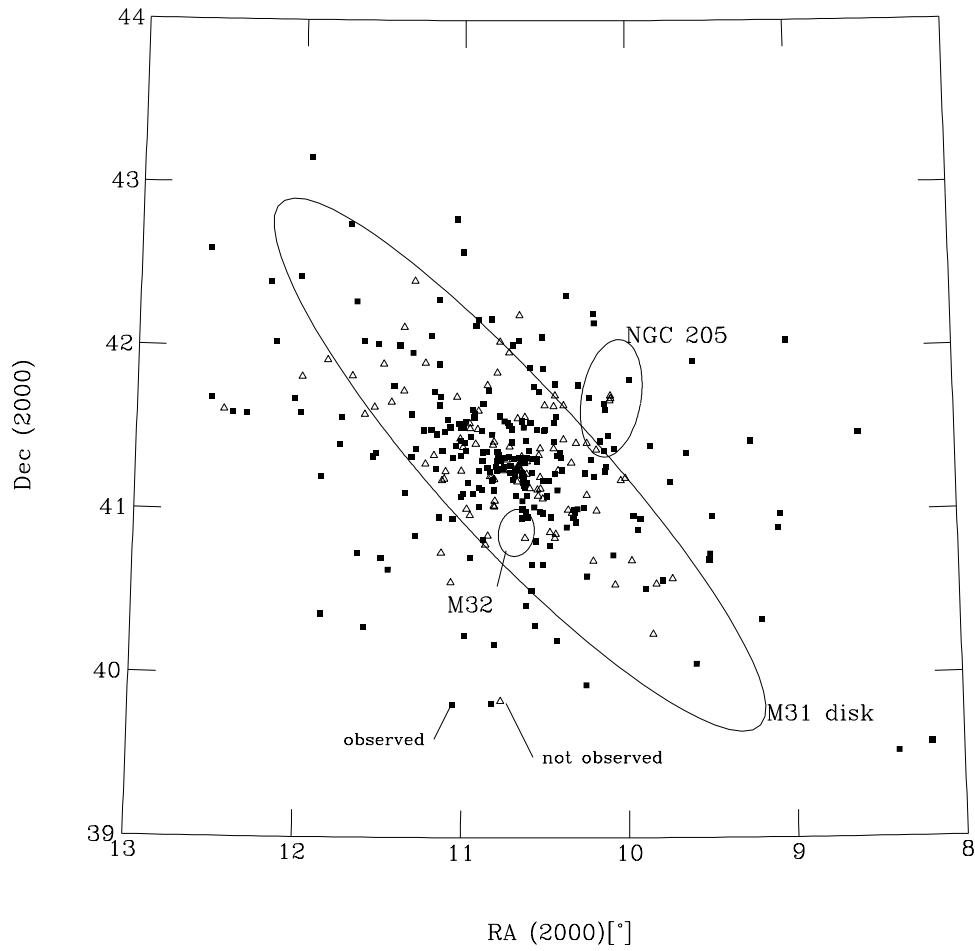


Fig. 1.— Photometric completeness for IR photometry (at least one of J , H , or K) of M31 GCs. Symbols indicate whether an object has been observed.

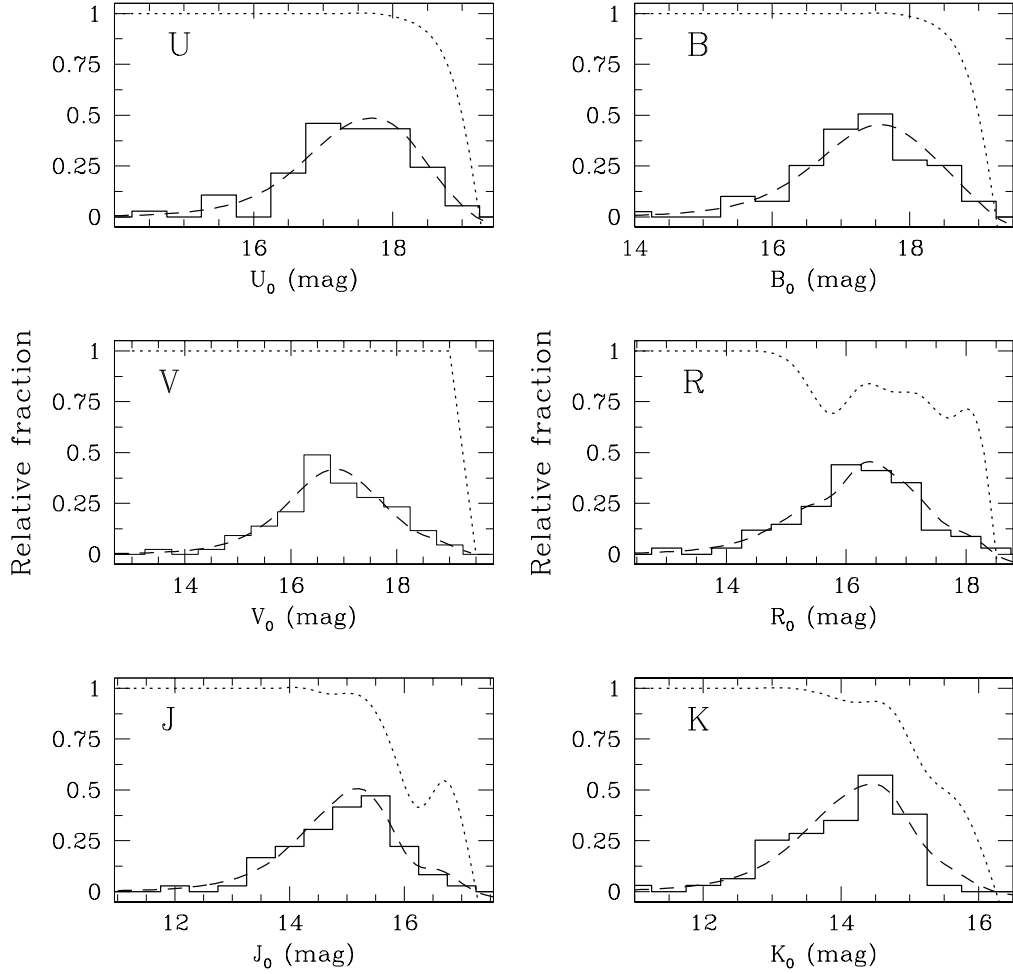


Fig. 2.— GCLFs and completeness functions for M31 halo clusters. The dip in the R -band completeness function is real; five clusters with $16.25 < V < 16.75$ (estimated $15.5 < R_0 < 16.0$) do not have measured R magnitudes.

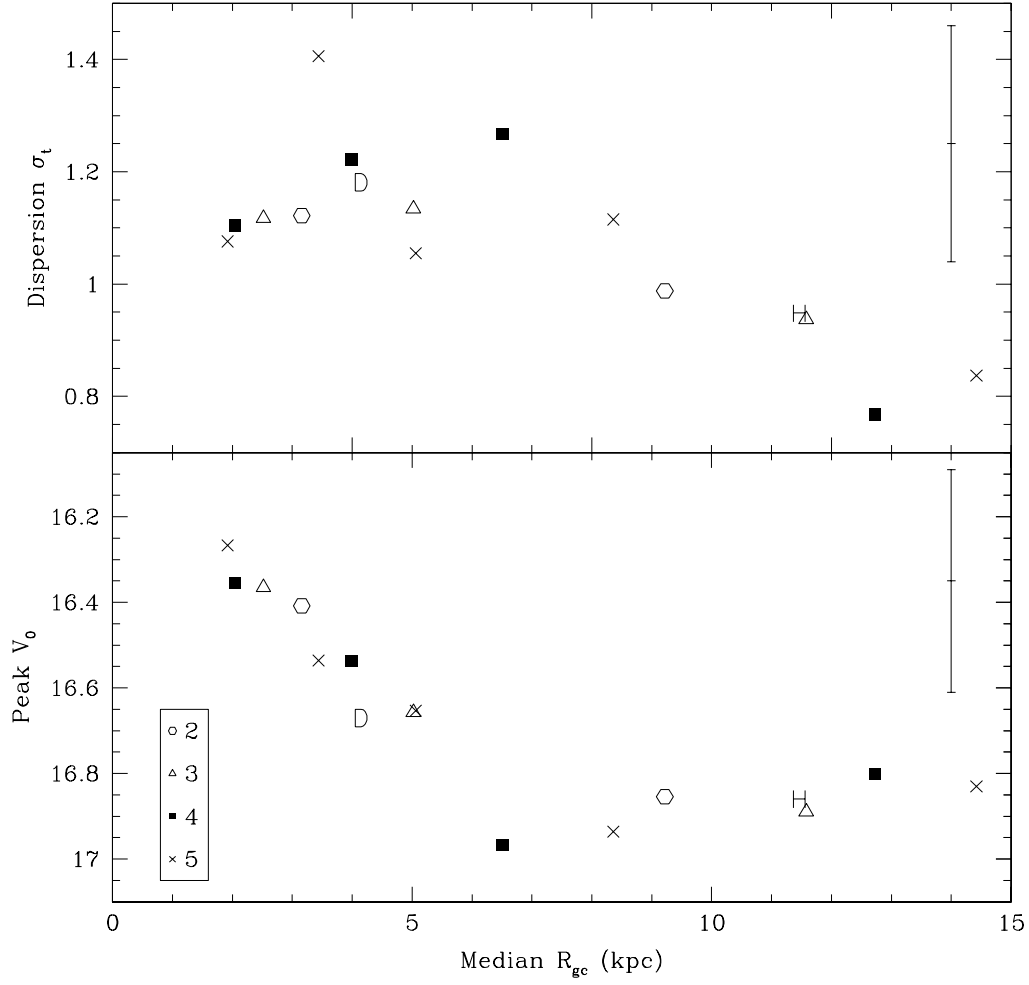


Fig. 3.— GCLF peaks and dispersions for groups of M31 clusters, sorted by projected distance from the center of M31. The different symbols represent the division of the GCS into different numbers of groups; ‘D’ and ‘H’ show the location of the disk and halo samples.

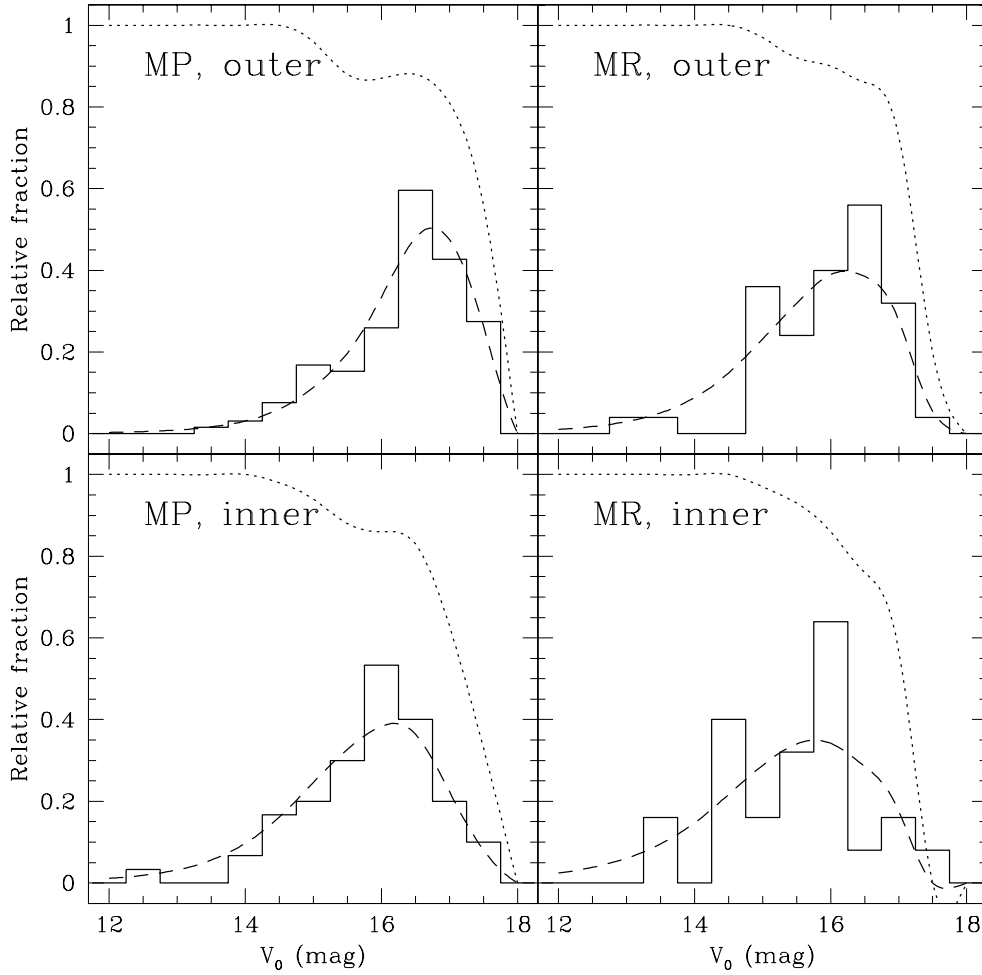


Fig. 4.— GCLFs and completeness functions for four groups of M31 GCs: (a) MP, outer (b) MR, outer (c) MP, inner (d) MR, inner. The dip in the completeness function for the MP clusters is due to the presence of a few bright objects without metallicities (likely to be metal-poor because MP clusters make up two-thirds of the population).

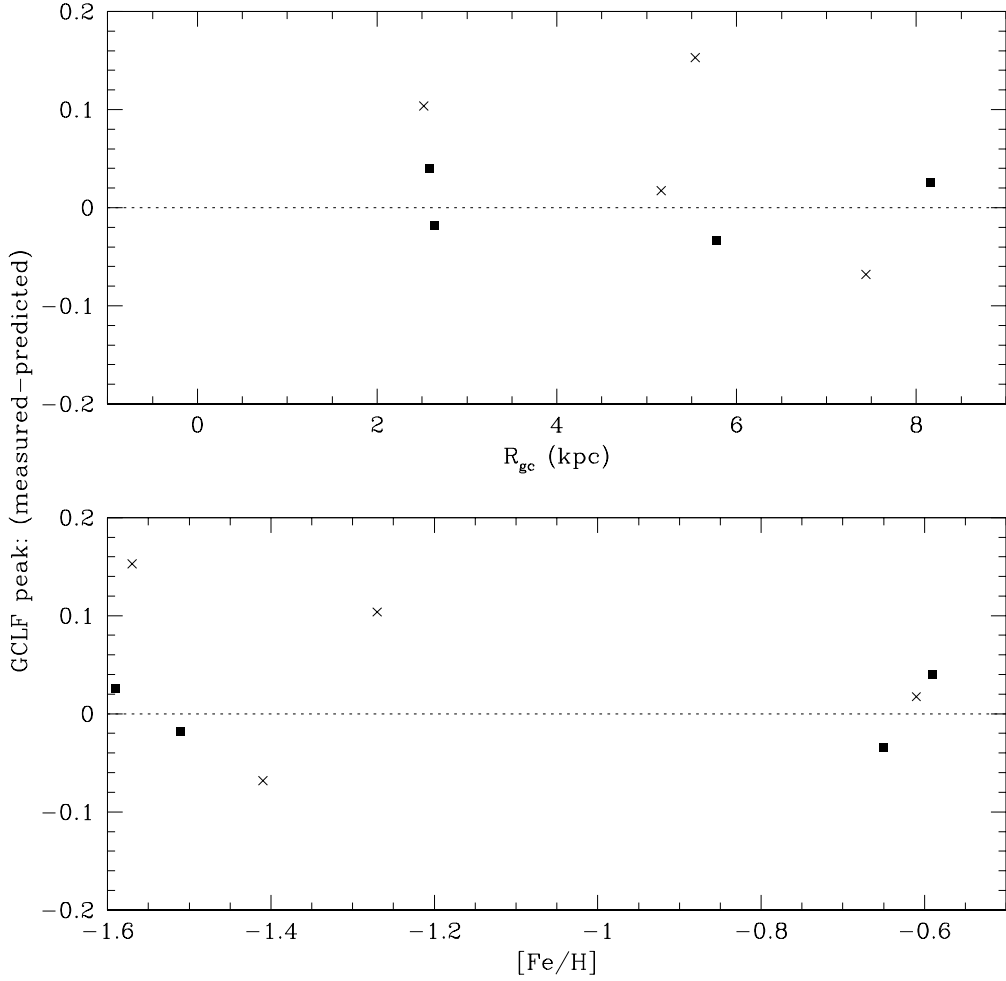


Fig. 5.— Difference between predicted (from Equation 6) and measured GCLF peaks for the data in Table 4. Crosses are data from the first four lines of the table, used in fitting the regression equation. Squares are data from the last four lines, which were not used in the regression because they are not independent samples of the M31 GC population.

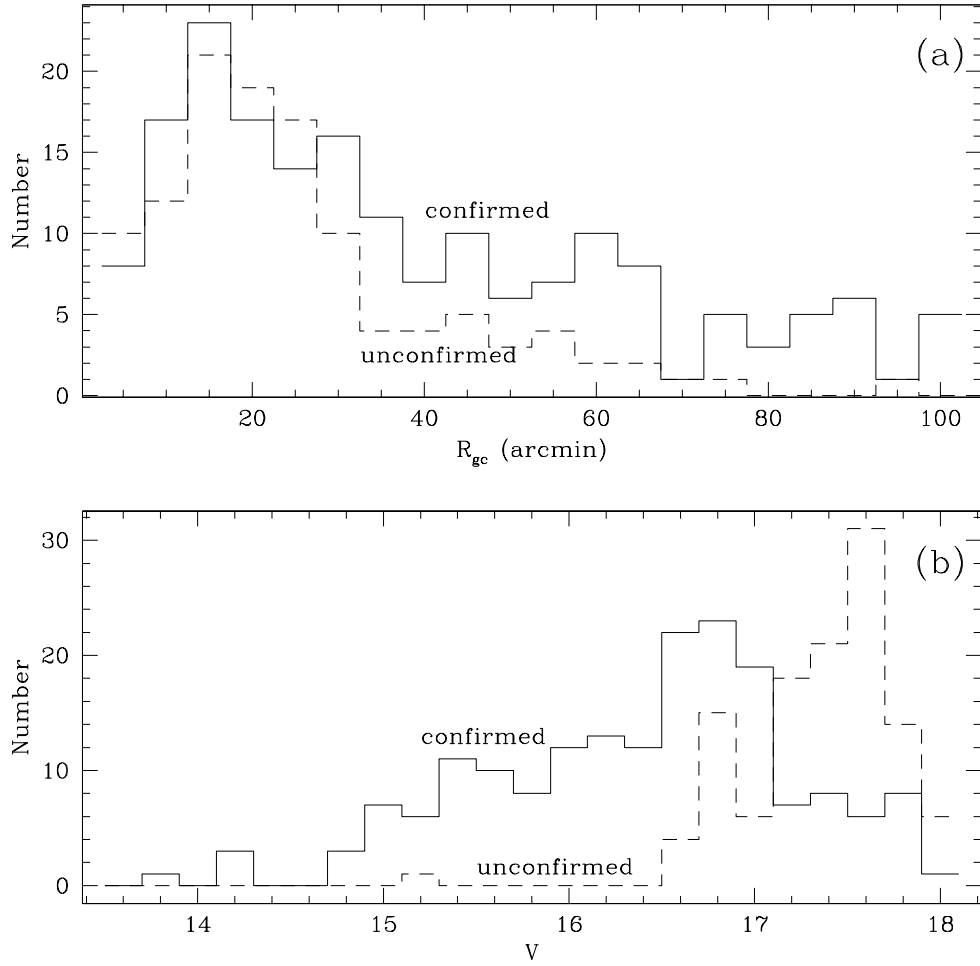


Fig. 6.— Distribution of R_{gc} and V for confirmed and unconfirmed M31 GCs. The fraction of confirmed clusters rises slowly with R_{gc} and drops rapidly with V .

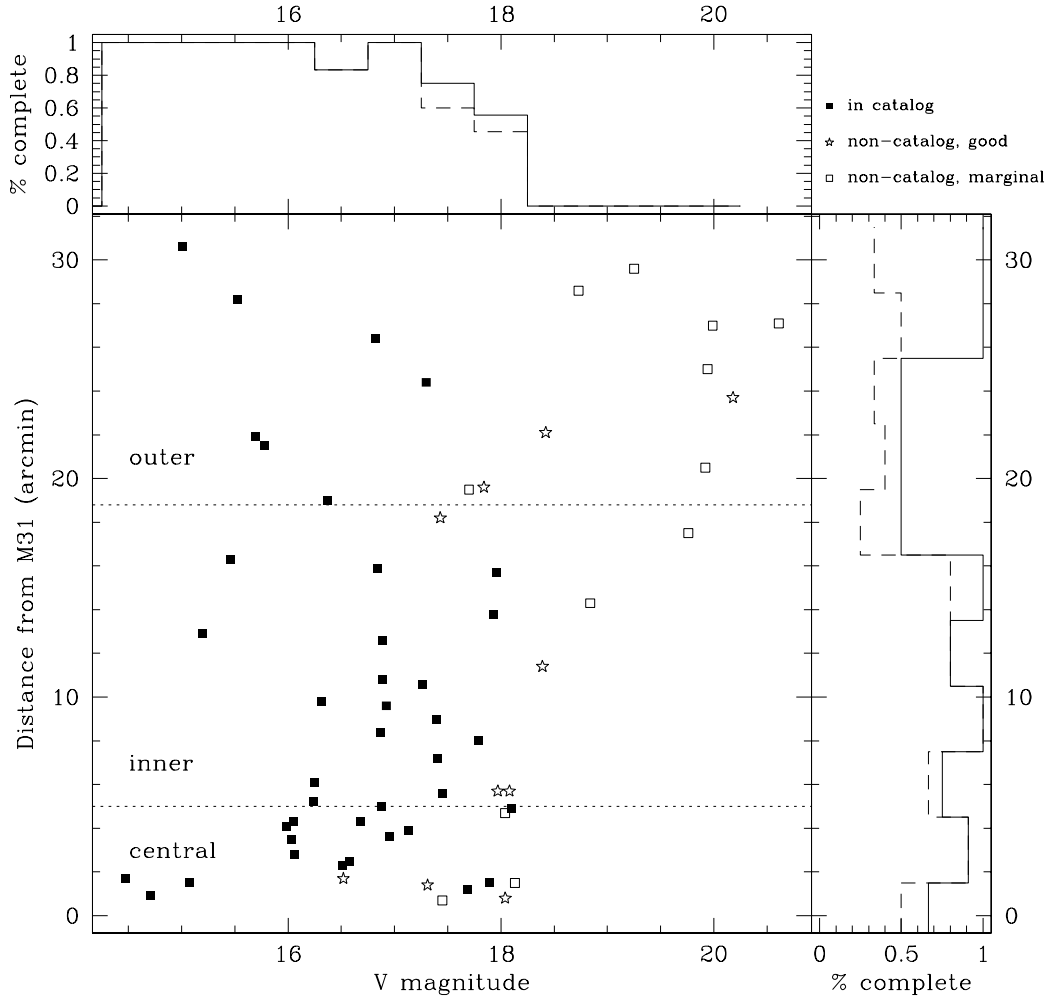


Fig. 7.— Distribution in R_{gc} and V for cluster candidates in HST fields. The catalog completeness as a function of R_{gc} and V is (number of cataloged clusters) divided by (total number of clusters); solid lines are the completeness computed using good GC candidates only and dashed lines include marginal candidates.